Crystal structure and activity of *Bacillus subtilis* YoaJ (EXLX1), a bacterial expansin that promotes root colonization

Frédéric Kerff[a,1], Ana Amoroso[a,1], Raphaël Herman[a], Eric Sauvage[a], Stéphanie Petrella[b], Patrice Filée[a], Paulette Charlier[a], Bernard Joris[a], Akira Tabuchi[c], Nikolas Nikolaidis[c,2], and Daniel J. Cosgrove[c,3]

[a]Université de Liège, Centre d'Ingénierie des Protéines, Institut de Chimie B6, 4000 Liège, Belgium; [b]Laboratoire de Recherche Moléculaire sur les Antibiotiques, Faculté de Médecine Pitié Salpêtrière, 75013 Paris, France; and [c]Department of Biology, Pennsylvania State University, University Park, PA 16802

Contributed by Daniel J. Cosgrove, September 18, 2008 (sent for review August 6, 2008)

We solved the crystal structure of a secreted protein, EXLX1, encoded by the *yoaJ* gene of *Bacillus subtilis*. Its structure is remarkably similar to that of plant β-expansins (group 1 grass pollen allergens), consisting of 2 tightly packed domains (D1, D2) with a potential polysaccharide-binding surface spanning the 2 domains. Domain D1 has a double-ψ β-barrel fold with partial conservation of the catalytic site found in family 45 glycosyl hydrolases and in the MltA family of lytic transglycosylases. Domain D2 has an Ig-like fold similar to group 2/3 grass pollen allergens, with structural features similar to a type A carbohydrate-binding domain. EXLX1 bound to plant cell walls, cellulose, and peptidoglycan, but it lacked lytic activity against a variety of plant cell wall polysaccharides and peptidoglycan. EXLX1 promoted plant cell wall extension similar to, but 10 times weaker than, plant β-expansins, which synergistically enhanced EXLX1 activity. Deletion of the gene encoding EXLX1 did not affect growth or peptidoglycan composition of *B. subtilis* in liquid medium, but slowed lysis upon osmotic shock and greatly reduced the ability of the bacterium to colonize maize roots. The presence of EXLX1 homologs in a small but diverse set of plant pathogens further supports a role in plant–bacterial interactions. Because plant expansins have proved difficult to express in active form in heterologous systems, the discovery of a bacterial homolog opens the door for detailed structural studies of expansin function.

family 45 endoglucanase | lytic transglycosylase | peptidoglycan | plant cell wall | plant-microbe interactions

Bacterial and plant cell walls have similar functions but distinctive structures. Bacterial peptidoglycan forms a network of linear polysaccharide strands of alternating *N*-acetylglucosamine (GlcNAc) and *N*-acetylmuramic acid (MurNAc) residues cross-linked by short polypeptides. As a giant bag-shaped sacculus, peptidoglycan expands via the action of endopeptidases, amidases, and lytic transglycosylases that cleave covalent bonds and allow insertion of new subunits (1). In contrast, the growing plant cell wall is formed from a scaffold of cellulose microfibrils tethered together by branched glycans such as xyloglucan or arabinoxylan that bind noncovalently to cellulose surfaces. The cellulose–hemicellulose network enlarges via polymer slippage or "creep," mechanically powered by turgor-generated forces in the cell wall and catalyzed by expansins and other wall-loosening agents (2).

Expansins are known principally from plants where they function in cell enlargement and other developmental events requiring cell wall loosening (3). Canonical expansins are small proteins (≈26 kDa, ≈225 aa) consisting of 2 compact domains: D1 has a fold similar to that of family 45 glycosyl hydrolases (GH45), and D2 has a β-sandwich fold. Expansins facilitate cell wall creep without breakdown of wall polymers (3–5). Plant expansins consist of 2 major families: α-expansins, which preferentially loosen the cell walls of dicots compared with cell walls from grasses, and β-expansins, where the reverse is true. This selectivity presumably relates to the different matrix polysaccharides in the 2 types of cell walls (6).

Massive genomic sequencing in recent years has uncovered numerous gene sequences closely or distantly related to plant expansins (3, 7). Of particular interest for the current work are gene sequences that show up in BLAST searches with expansin as query and are found in a small set of phyllogenetically diverse bacteria, sometimes as part of modular endoglucanases. Alignments between these bacterial proteins and plant expansins show ≈15% identity distributed throughout the protein, suggestive of a similar structure, but lacking the expansin signature motifs. In this work, we determined the structure and activities of one of these proteins from *Bacillus subtilis*, a Gram-positive soil bacterium able to colonize the surface of plant roots (8). Our results reveal a protein remarkably similar to plant expansin and suggest that the *Bacillus* protein functions to promote root colonization.

Results

EXLX1 Has an Expansin Structure. The mature protein encoded by the *yoaJ* gene from *B. subtilis* was expressed in the periplasm of *Escherichia coli*. Crystals of the purified protein and its selenomethionine (SeMet) derivative appear in a sodium formate solution and belong to the body-centered cubic space group I23. Data collected with a single crystal of SeMet protein were used to solve and refine the structure to 2.5-Å resolution with an R_{cryst} of 0.203 and an R_{free} of 0.231. Higher resolution data (1.9 Å) were obtained with crystals of native protein with final R_{cryst} and R_{free} of 0.165 and 0.19, respectively [see supporting information (SI) Table S1]. For reasons given below, we refer to this protein as EXLX1, following expansin nomenclature (9).

EXLX1 is a 23-kDa protein made of 2 domains packed against each other to form a 60-Å long and 37-Å wide ellipsoid (Fig. 1*A*). The first domain (D1, residues 1–108) contains 3 α-helices and 6 β-strands forming a 6-stranded double-ψ β-barrel, found in domains from several protein families (10). The second domain (D2, residues 113–208) is organized in 2 sheets of 4 antiparallel

Author contributions: P.C., B.J., and D.J.C. designed research; F.K., A.A., R.H., E.S., S.P., P.F., A.T., and N.N. performed research; A.T., N.N., and D.J.C. analyzed data; and F.K., A.A., P.C., N.N., and D.J.C. wrote the paper.

The authors declare no conflict of interest.

Data deposition: The atomic coordinates and structure factors have been deposited in the Protein Data Bank, www.pdb.org (PDB ID codes 2BH0 and 3D30).

[1]F.K. and A. A. contributed equally to this work.

[2]Present address: Department of Biological Science, California State University, Fullerton, CA 92834.

[3]To whom correspondence should be addressed at: 206 Life Science Building, Pennsylvania State University, University Park, PA 16802. E-mail: dcosgrove@psu.edu.

This article contains supporting information online at www.pnas.org/cgi/content/full/0809382105/DCSupplemental.

© 2008 by The National Academy of Sciences of the USA

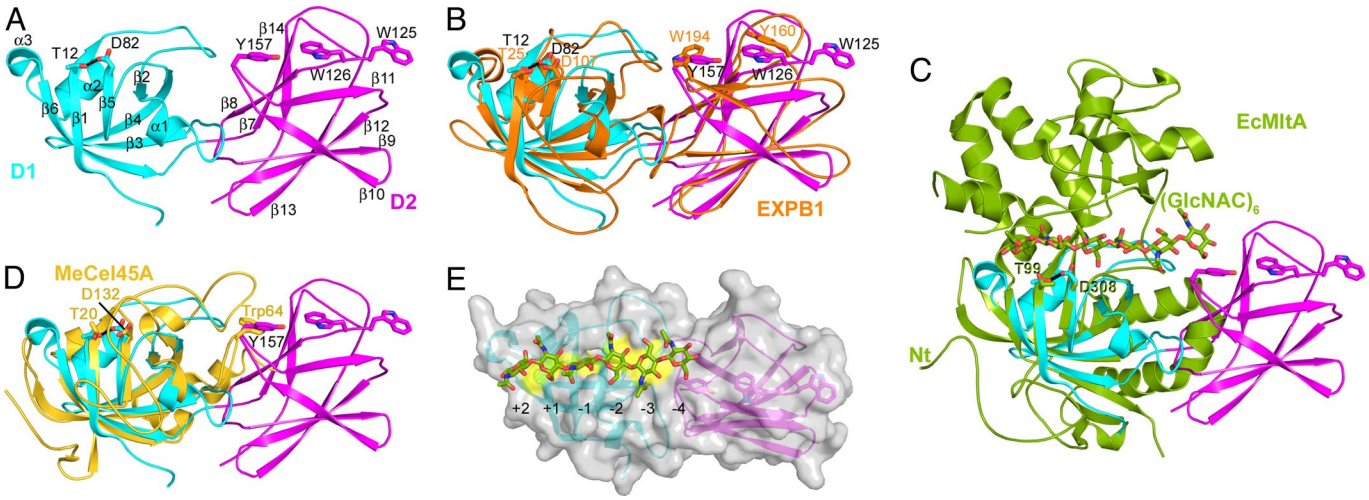

Fig. 1. Structure of EXLX1 and comparison with other proteins containing a double-ψ β-barrel fold and interacting with polysaccharides. (*A*) Diagram representation of EXLX1: D1, cyan; D2, magenta. (*B*) Diagram representations of EXLX1 and EXPB1 (orange) superimposed. (*C*) Diagram representations of EXLX1 and EcMltA(D308A)–chitohexaose superimposed. The chitohexaose [$(GlcNAc)_6$] is shown as sticks. Nt, N-terminal extension. (*D*) Diagram representations of GH45 endoglucanase MeCel45A and EXPB1 superimposed. (*E*) Diagram and surface representation of EXLX1 with chitohexaose (in sticks) from the superimposed EcMltA(D308A)–chitohexahose. The most conserved residues in proteins with a double-ψ β-barrel fold are highlighted in yellow. EXLX1 is oriented with shallow groove on the front instead of on top as in *A–D*.

strands, forming an Ig-like β-sandwich. Domains with this fold characteristically have a binding function, and in this context it is notable that 3 aromatic residues (Trp-125, Trp-126, Tyr-157) are aligned in a plane on the surface of D2 (Fig. 1*A*). The 2 domains are connected by a short linker (residues 109–112).

Structural neighbor analysis by the VAST algorithm (11) showed the most closely related structures to be β-expansins, exemplified by EXPB1 from maize pollen (5) and a timothy grass homolog named Phl p 1 (PDB codes 2HCZ, 1N10). These 2 proteins have plant cell wall extension activity (12) and are the only proteins in the VAST structure database that align structurally with both domains of EXLX1. Superposition of EXLX1 and EXPB1 using the secondary structure matching (SSM) algorithm (13) of the program Coot (14) shows them to be highly congruent (Fig. 1*B*), with a root mean square deviation (rmsd) of 2.3 Å for 186 residues. Superposition of the individual domains separately gives an rmsd of 1.9 Å for D1 (98 residues) and 1.6 Å for D2 (82 residues). Like EXPB1 (5), EXLX1 has a shallow planar surface that spans the 2 domains and that is lined with aromatic and polar residues suitable for polysaccharide binding. Two notable differences in structure between EXLX1 and the pollen β-expansins are (*i*) the absence in EXLX1 of a flexible N-terminal extension of 13 residues, and (*ii*) the lack in EXLX1 of disulfide bridges that are highly conserved features of the D1 expansin fold (5). We conclude that despite its low sequence similarity to expansins, EXLX1 has a canonical expansin structure, and we named it accordingly (9).

Structures Related to D1. A VAST search with D1 alone combined with bibliographical searches identified 4 structurally related families involved in polysaccharide recognition: the plant defense protein barwin (15), GH45 (3, 16–18), plant expansins (3), and family 2 of peptidoglycan lytic transglycosylases (LT), exemplified by MltA (19). LTs cleave the β1,4-glycosidic bond between MurNAc and GlcNAc with the concomitant formation of a 1,6-anhydro ring at the MurNAc residue, which thereby becomes a nonreducing sugar. With the SSM algorithm we superposed the crystallographic structures of 9 proteins: 3 expansins (*B. subtilis* EXLX1; maize EXPB1; Phl p 1); 3 family 2 LTs [EcMltA from *E. coli*, Protein Data Bank (PDB) ID code 2AE0 (20, 21); AtMltA from *Agrobacterium tumefaciens*, PDB ID code 2PNW; NgMltA from *Neisseria gonorrhoeae*, PDB ID code 2G5D]; and 3 GH45 structures [MeCel45A from *Mytilus edulis*, PDB ID code 1WC2; HiCel45 from *Humicola insolens*, PDB ID code 2ENG (16); MaCel45 from *Melanocarpus albomyces*, PDB ID code 1OA9 (18)]. These proteins are quite divergent: pairwise sequence alignments with D1 range from 8% to 35% identity for most pairs (Table S2). The domain structures also differ. The 3 MltA enzymes do not have a domain equivalent to D2 but do have an N-terminal extension of 80–130 aa packed on D1 and an additional domain (140–200 aa) inserted after β-strand β1 (Figs. 1*C* and 2). This domain has a different spatial relationship with D1 compared with D2. The 3 GH45 enzymes likewise do not contain a D2 domain and can be divided into 2 subgroups: MeCel45A is a compact structure with short loops between β-strands (Fig. 1*D*), whereas HiCel45 and MaCel45 have 2 large insertions ($\approx$50 aa), one in the $\beta1\beta2$ loop and another in the $\beta5\beta6$ loop (Fig. 2 and Fig. S1). Superposition of these proteins shows that the GH45 and MltA domains are equally distant from D1 of EXLX1 (rmsd values of 2.0 to 2.3 Å and 1.9 to 2.6 Å, respectively; Table S2). The most closely related of these structures is MeCel45A with a rmsd of 2.0 Å for 89 residues and 18% identity.

The sequence alignment based on the 9 superposed structures shows only 2 strictly conserved residues (highlighted in cyan in Fig. 2), a threonine and an aspartic acid (Thr-12 and Asp-82 in EXLX1). Asp-82 is located on β5 and is equivalent to the single catalytic Asp identified in LT enzymes (Asp-308 in EcMltA) and to 1 of the 2 catalytic residues in GH45 enzymes (Asp-132 in MeCel45A). The equivalent residue is also conserved in plant expansins (3). Thr-12 is located on β1, and its hydroxyl group is involved in a conserved hydrogen bond with the carboxylic group of Asp-82. The equivalent Thr is likely important for the proper positioning of the catalytic Asp in MltA and GH45. In the high resolution (1.2 Å) MeCel45A structure, the 2 equivalent residues (Thr-20 and Asp-132) are found in 2 conformations. One conformation is similar to that observed in all of the superposed structures, whereas in the second conformation Asp-132 makes a hydrogen bond with His-130. This histidine is also relatively well conserved (Fig. 2). The flexibility of this Asp may therefore be important for its catalytic function. Nine other residues are conserved in at least two-thirds of these crystal structures

BIOCHEMISTRY

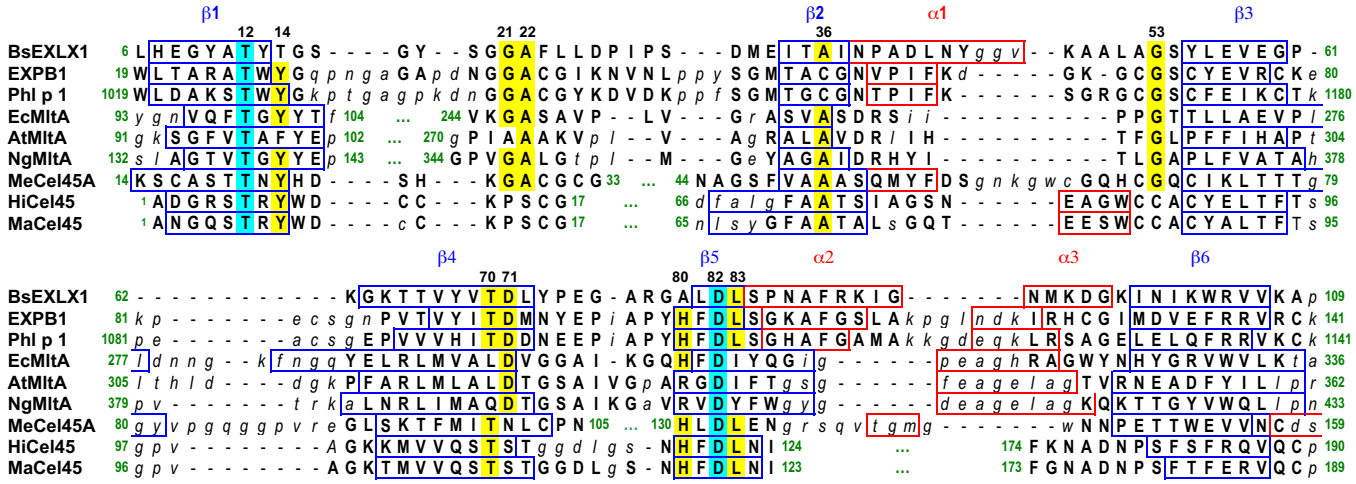

Fig. 2. Sequence alignment of D1 of EXLX1 with 2 other expansins, 3 LTs, and 3 GH45s. Structurally aligned residues are displayed in capital letters, strictly conserved residues are highlighted in cyan, and residues conserved in two-thirds of the structures are in yellow. β-Strands and α-helices are marked with blue and red boxes, respectively.

(highlighted in yellow in Fig. 2), and 7 exist in EXLX1. With the exception of Gly-53, all of these residues are part of the D1 portion of the shallow groove that potentially serves as a polysaccharide-binding site (Fig. 1*E*). Two of these residues surround the catalytic Asp in MltA and GH45, further emphasizing the importance of this strictly conserved residue (Asp-82 in EXLX1).

Superposition of EXLX1 D1 with the EcMltA–chitohexaose complex (21) shows that this chitin fragment would fit very well in the shallow groove of EXLX1 D1 (Fig. 1*E*), and most of the interactions between chitohexaose and D1 of EcMltA are potentially conserved in EXLX1 (Fig. S2). However, the binding site of EcMltA is a deep cleft at the interface of the 2 domains (Fig. 1*C*), and there are no equivalents in EXLX1 for the interactions with the additional EcMltA domain.

EXLX1 was also compared with a HiCel45–cellohexaose complex (16), where 2 β1,4-glucan fragments are bound to the active site. Three of 4 hydrogen bonds with the substrate are predicted to be conserved in EXLX1. The 2 large insertions in HiCel45 play a role similar to the additional domain of EcMltA, providing hydrogen bonds and hydrophobic interactions on the other side of the active-site cleft (Fig. S1). Most of these hydrophobic interactions are absent in MeCel45A and in EXLX1. The active-site cleft of MeCel45A is intermediate between the shallow groove of EXLX1 and the long deep cleft of the MltA and the 2 other GH45 structures.

From the superposition of EXLX1 with the EcMltA–chitohexaose and HiCel45–cellohexaose complexes, it seems that the 3 aromatic residues on the D2 surface are well positioned to extend the potential binding surface of D1 in EXLX1 (Fig. 1*C* and Fig. S1), binding up to 4 additional saccharide units.

D2-Related Structures. Structures closely related to D2 include the group 2/3 grass pollen allergens (PDB codes 1WHO, 2JNZ) that are evolutionary descendants of the D2 domain of β-expansins (3, 7). A β-sandwich with 3–6 strands per sheet is the most common fold for a carbohydrate-binding module (CBM) (22), which often contains 1 or more bound calcium ions involved in protein stability and ligand binding. EXLX1 does not have metal ions bound to D2. CBMs are also classified according to their function or substrate type. With 2 tryptophans and 1 tyrosine making a planar platform of aromatic residues (Fig. 1*A*), D2 resembles a type A CBM, some of which are specific for crystalline cellulose or chitin.

Cell Wall Loosening Activity. In view of its structural similarity to plant expansins, we tested EXLX1 for its ability to induce extension of plant cell walls, the standard assay for expansin activity (3). EXLX1 induced a small, but significant, rate of extension in cell walls from wheat coleoptiles (Fig. 3) but not cucumber hypocotyls. Such activity is characteristic of expansins, with selectivity toward grass walls being typical of β-expansins such as maize EXPB1 (23). However, the activity of EXLX1 was weak compared with EXPB1. For example, an EXLX1 concentration of 250 μg/mL was required to induce an extension rate of 2.2% h^{-1} (Fig. 3 *Inset*), whereas 25 μg/mL EXPB1 induced an equivalent extension rate. We also found a marked synergism between EXLX1 and EXPB1 activity. Pretreatment of coleoptile walls with 5 μg of EXPB1 amplified the subsequent response to EXLX1 (Fig. S3). A similar enhancement was seen when EXPB1 followed EXLX1 exposure. One interpretation of this synergism is that EXLX1 and EXPB1 cause slippage of different load-bearing polymers in the grass cell wall. When applied together, the wall extension response would then be more than additive. We conclude from these experiments that EXLX1 has weak expansin activity, potentially acting on a different wall component than does EXPB1.

EXLX1 was also tested for its ability to cause mechanical weakening of cell walls, measured as stress/strain behavior, but

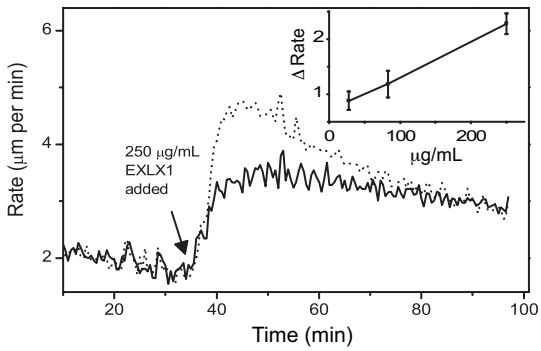

Fig. 3. Cell wall loosening activity of EXLX1. Two representative examples are shown of EXLX1-induced extension in heat-inactivated wheat coleoptile walls. (*Inset*) Dependence of induced extension rate (micrometers per minute) on applied EXLX1 concentration (micrograms per milliliter). The points are means ± SEM of 8–12 replicates.

no mechanical weakening was found (Fig. S4). Induction of cell wall extension without mechanical weakening is characteristic of α-expansin action (24).

Binding to Plant and Bacterial Cell Wall Polymers. With an applied concentration of 40 μg/mL, EXLX1 bound to plant cell walls, to pure cellulose, and to insoluble peptidoglycan from *B. subtilis* (Fig. S5). Because EXLX1 is a basic protein (calculated pI = 9.35), it is not surprising that it binds to plant cell walls or peptidoglycan, which contain acidic sugars. Inclusion of 10 mM $CaCl_2$ in the buffer substantially reduced EXLX1 binding to plant cell walls and to cellulose, indicating a substantial ionic component in these binding interactions. In contrast, 5 M NaCl did not release EXLX1 from peptidoglycan; heating in 2% SDS and digestion by lysozyme were needed to release EXLX1 bound to peptidoglycan. These results indicate a substantial nonionic component of EXLX1 binding to peptidoglycan, in contrast to a major ionic component of binding to plant cell walls and cellulose.

Lytic Activities. In view of its binding properties and its structural similarities to GH45 and LT, we tested EXLX1 for lytic activities against plant cell wall polysaccharides and peptidoglycan. No reducing sugars or UV-absorbing substances (e.g., ferulated arabinoxylans) were released from heat-inactivated wheat coleoptile walls incubated with EXLX1, indicating negligible cell wall hydrolytic activity. Polysaccharide lysis was also assessed by dye release from dye-coupled cross-linked polysaccharides, a very sensitive assay for endo-type lytic activities. Eight different substrates, representing the major polysaccharides of the grass cell wall, were incubated for 24 h with 6 μM EXLX1, essentially with negative results (Fig. S6*A*). Trace activities were detected with β(1–3, 1–4)D-glucan and hydroxyethylcellulose, suggesting that EXLX1 has vestigial β(1–4)-endoglucanase activity. However, the activity was exceptionally low and could come from trace contamination of EXLX1 with *E. coli* endoglucanases. For instance, 3 ng of a *Trichoderma* cellulase preparation had the same lytic activity as 27 μg of EXLX1 in these assays. Because cellulase makes up <10% of the commercial preparation, we estimate the specific activity of the purified EXLX1 solution to be $\approx 10^5$-fold lower than that of *Trichoderma* cellulase. With these 2 β-glucan substrates we also tested for endotransglucosylase activity, e.g., analogous to xyloglucan endotransglucosylase (25), but with negative results (Fig. S6). EXLX1 did not hydrolyze crystalline cellulose (Avicel), nor did it enhance cellulose hydrolysis in the presence of low levels of added cellulase beyond that observed for BSA used as a nonspecific control (Fig. S6*B*).

Lysis of peptidoglycan was analyzed by reverse-phase HPLC before and after incubation with EXLX1, but no lytic activity was detected. We conclude from these series of experiments that EXLX1 has no significant lytic activities with these plant and bacterial cell wall substrates under the tested conditions.

Phenotype of the EXLX1 Mutant. We compared the characteristics of wild-type *B. subtilis* with an EXLX1$^-$ mutant with respect to cell growth, separation of daughter cells during cell division, and autolysis. No difference in generation time was observed when cells were grown in liquid Luria–Bertani medium, and no change of morphology was observed by phase-contrast microscopy, indicating that the protein is not essential for normal cell growth under these conditions. HPLC analysis did not reveal differences in the structural pattern or amount of muropeptides in the wild type and EXLX1$^-$ mutant, suggesting that EXLX1 does not modify peptidoglycan composition.

The EXLX1$^-$ mutant had a slightly slower rate of cell autolysis (Fig. 4*A*), induced after cells were centrifuged and resuspended in buffer. In these conditions, a deenergization of cells leads to imbalanced peptidoglycan metabolism, triggering autolysis (26).

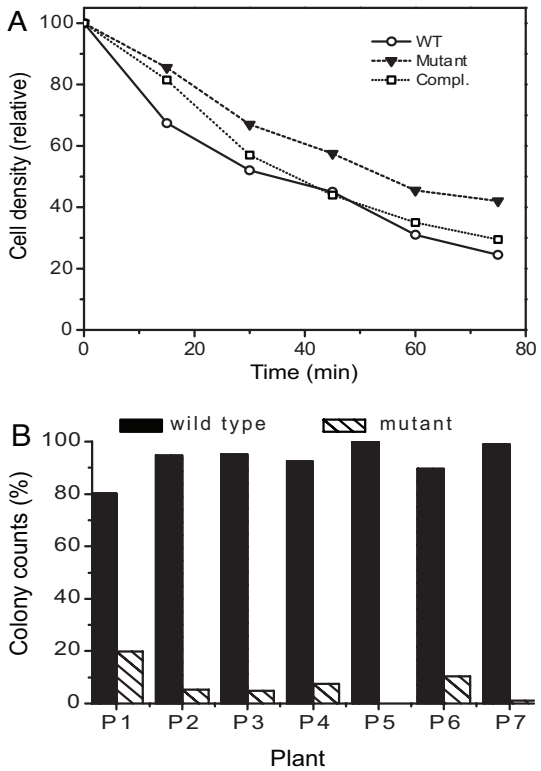

Fig. 4. Phenotypes of the EXLX1$^-$ mutant. (*A*) Autolysis curves for *B. subtilis* wild type (○), EXLX1$^-$ mutant (▼), and complemented mutant (□). Results are representative of 3 independent experiments. (*B*) Colonization rate of maize roots by wild-type *B. subtilis* versus the EXLX1$^-$ null mutant. Values are expressed as percentage of total bacterial counts in 7 replicates (P1–7).

The wild-type phenotype was restored when the mutant was complemented with a plasmid containing the complete *yoaJ* gene with its native promoter region to ensure a similar protein expression (verified by Western blotting). This subtle phenotypic difference was also seen when various agents known to promote autolysis in *B. subtilis* (27) were added to the buffer, including detergents, dissipaters of proton motive force, antibiotics, pH, and muramidases (data not shown). These results suggest that EXLX1 promotes peptidoglycan breakdown during induced autolysis, but the mechanism and its importance are unclear.

EXLX1$^-$ and wild-type *B. subtilis* were also assessed for their ability to colonize plant roots. Sterile maize roots were inoculated with 1:1 mixtures of wild-type and mutant *B. subtilis*, and a census of bacteria bound to the root surface was made after 3 days. Root colonization was greatly reduced in the EXLX1$^-$ mutant compared with wild type (Fig. 4*B*). We conclude that EXLX1 promotes root surface colonization by *B. subtilis*.

Discussion

Our results show that EXLX1 shares major structural features and activities with plant expansins, including its 2-domain structure, the precise spatial alignment of the 2 domains resulting in an open binding surface spanning the 2 domains, protein binding to cell walls, induction of plant cell wall extension without mechanical weakening, and lack of lytic activity against major polysaccharides of the plant cell wall. Plant cell wall extension activity is a unique hallmark of expansin action, and for this reason, as well as its structural similarity to plant expansins, we consider this protein to be a member of the expansin superfamily. Its wall extension activity is very weak, however, which could mean that EXLX1 function requires muted extension activity or that wall extension activity is incidental to its primary function.

BIOCHEMISTRY

In nature, *B. subtilis* colonizes plant roots (8); and in agriculture, this bacterium is used as a biocontrol agent against fungal pathogens (28). Our discovery that EXLX1 promotes bacterial colonization of maize roots suggests that its biological role is to enhance plant–bacteria interaction.

This inference gains additional support from BLAST analyses of public databases by using EXLX1 as query, which identify several closely related proteins (identity >72%; E-value $<10^{-67}$) from *Xanthomonas*, *Xylella*, *Ralstonia*, and *Erwinia* (Table S3). These are phyllogenetically diverse bacteria, classified as Firmicutes, γ-proteobacteria, and β-proteobacteria. Notably, they are serious plant pathogens, and most of them live and propagate in the water-conducting xylem of the vascular system. The presence of EXLX1 homologs in diverse plant pathogens, but not in other closely related bacteria that are not plant pathogens, supports our conclusion that EXLX1 functions in plant–bacteria interactions. Not all bacteria with important plant interactions have an EXLX1 homolog, however. For instance, EXLX1 homologs were not identified in the genomes of *Agrobacterium*, *Rhizobium*, or *Pseudomonas*, i.e., bacterial species involved in pathogenic or symbiotic relationships with plants. We infer from these results that EXLX1 homologs are likely involved in plant colonization by many, but not all, bacteria that interact with plants.

In a related vein, a modular endoglucanase with a domain distantly related to EXLX1 was found to be an important virulence factor for inducing symptoms during infection of tomato plants by *Clavibacter michiganensis* (29, 30). Likewise, a recent study found that overexpression of "swollenin," a fungal protein with an expansin-like domain, enhanced benign colonization of cucumber roots by *Trichoderma reesei* (31). These reports, combined with our results, suggest that expansin-type modules have been adapted by diverse microbes to facilitate their interactions with plants, whether for benign colonization as in *B. subtilis* and *T. reesei* or for pathogenic attack as in *C. michiganensis* or the other plant pathogens noted above.

The molecular basis by which EXLX1 promotes colonization is uncertain. Its strong binding to peptidoglycan suggests that it is anchored to the bacterial surface, but its actual location is unknown. EXLX1 might promote subtle modification of the plant cell wall, perhaps aiding plant cell wall breakdown by enzymes secreted by *B. subtilis* (32). A similar synergism between EXLX1 and peptidoglycan hydrolases could also explain the slightly more efficient autolysis of wild-type *B. subtilis* compared with the EXLX1$^-$ mutant. Another possibility is that EXLX1 participates in formation or modification of bacterial biofilms, formed during root colonization. A third possibility is that EXLX1 acts as a bifunctional binding agent, binding peptidoglycan and the plant cell wall surface simultaneously, perhaps separately via the 2 domains. This dual binding could induce a "hinging" of D1 and D2 as proposed for the wall loosening activity of plant expansins (5). With a contact area of 986 Å^2, the surface of interaction between the 2 domains is small (33) and therefore could change upon saccharide binding. Such a model for EXLX1 action is compatible with Gram$^+$ bacteria like *B. subtilis* in which direct contact between peptidoglycan and the root cell wall is possible, but a similar mechanism in Gram$^-$ bacteria like proteobacteria would be prevented by the outer membrane.

The binding of EXLX1 to peptidoglycan has a large nonionic component, whereas its binding to plant cell wall and cellulose has a large ionic component. The latter interaction may therefore be reduced in saline soils. From the superposition of D1 of EXLX1 with the GH45 and MltA structures, several conserved residues in EXLX1 were identified that likely contribute to its binding to these complex polysaccharides. The structures, however, are of no help in predicting the relative affinity for these materials. The contribution of D2 to binding is also hard to evaluate at this time because oligosaccharide–protein complexes are not yet available for D2. Structurally, D2 is similar to type A CBMs that are specific for more crystalline polysaccharides such as pure cellulose (22). Thus, D2 may be more important for EXLX1 binding to cellulose and to plant cell walls than to peptidoglycan, which is not crystalline.

For MltA, a 2-step mechanism is proposed for peptidoglycan cleavage, with a single Asp residue playing the central role in both steps (21). In the first step, it acts as an acid, attacking and cleaving the glycosidic bond; and in the second step, it acts as a base, activating the hydroxyl group of MurNAc to induce the formation of the 1,6-anhydroMurNAc product. This Asp is equivalent to the general acid in GH45 (Asp-121 in HiCel45) and to the conserved Asp of expansins (Asp-82 in EXLX1). It is found in an identical orientation in the 9 related crystal structures compared in this article. However, in the LT mechanism, the positions of the substrate and the reaction intermediates in the catalytic cleft have to be stabilized by other elements of this enzyme for catalytic activity. EXLX1, and plant expansins, lack the additional domain that completes the catalytic cleft of MltA. This may account for the lack of lytic activity in EXLX1 and in plant expansins (5, 34). Thus, the structural similarity between expansin and MltA, first noted by van Straaten *et al.* (20), does not mean similar catalytic activity. The D2 domain could potentially increase substrate binding, but its distance from the potential lytic site means it is unlikely to stabilize a LT reaction.

Whatever its mechanism of action, the importance of EXLX1 for root colonization makes it a very good candidate for further work to improve the efficiency of *B. subtilis* and other organisms as biocontrol agents. Furthermore, because plant expansins have proved difficult to express in active form in heterologous expression systems, the discovery of a bacterial expansin opens the way for molecular engineering of the EXLX1 scaffold to elucidate the structural requirements for expansin activity.

Materials and Methods

Strains and Culture Media. *B. subtilis* 168 1AI (Bs), Trp- (Bacillus Genomic stock center, Ohio State University, Columbus, OH) was used for genomic DNA and bacterial physiological studies. An EXLX1$^-$ (*yoaJ*) mutant was created by gene interruption with a Tn10-Spc cassette (see *SI Materials and Methods*) and was used for bacterial physiological studies. A second mutant, used for the root colonization experiments, was produced by insertional mutagenesis of *B. subtilis* (strain 168) with the pMUTIN plasmid (35).

Protein Expression and Purification. The *yoaJ* gene was inserted into pET22b (Novagen) and expressed in *E. coli* strain BL21 (DE3-pLys). Replacement of the original signal peptide by the *pelB* signal peptide in pET22b results in an extra methionine at the N terminus. *E. coli* strain B834(DE3), auxotrophic for methionine, was used to express the SeMet derivative. For details of protein purification, see *SI Materials and Methods*.

Crystallization, Data Collection, Structure Solution, and Refinement. EXLX1 was concentrated to 46 mg/mL and crystallized at 20 °C by hanging-drop vapor diffusion, and diffraction data were collected at the BM30A beamline of the European Synchrotron Radiation Facility. The single-wavelength anomalous diffraction method was used to solve the SeMet protein structure with a 2.5-Å resolution dataset collected at the Se absorption edge. All of the aa of the protein are modeled in the final structure, except the N-terminal SeMet. A 1.9-Å resolution model was obtained with the native (non-SeMet) protein. For details, see *SI Materials and Methods*.

Plant Cell Wall Extension. Heat-inactivated cell wall specimens from cucumber hypocotyls (representing dicot cell walls) or wheat coleoptiles (representing grass cell walls) were prepared as described in ref. 5, clamped in a constant-force extensometer at 20-gram force in 50 mM sodium acetate (pH 5.5). Specimen length was recorded at 30-s intervals (23, 36) before and after addition of recombinant EXLX1 or native EXPB1 purified from maize pollen (37).

Cell Autolysis Assays. Cells were grown overnight at 37 °C with shaking in a small volume of LB. Precultures were diluted 1:100 in 100 mL of the same medium, and cultures were grown to an optical density of 0.6–0.7 (600 nm), chilled on ice, and centrifuged at 7,000 × *g* for 5 min. Cells were washed 3 times with 0.9 g/L NaCl and resuspended in 20 mL of 100 mM phosphate buffer

(pH 7), and incubated with gentle shaking at 37 °C. Lysis was measured as the decrease in absorbance at 575 nm.

Root Colonization. This assay was adapted from Yaryura *et al.* (38), as detailed in *SI Materials and Methods*. In brief, *Zea mays* seeds were surface-sterilized, germinated for 2 days in the dark, transferred to culture tubes containing 5 mL of mineral solution and filter paper as mechanical support of the seedling, and inoculated with equal amounts of wild-type and mutant cells. After growth for 3 days, a census of cells attached to the roots was made. Wild-type cells carried a plasmid expression of green fluorescent protein (GFP), permitting visual distinction between wild-type and mutant colonies. Control experiments showed that the GFP plasmid slowed *B. subtilis* growth in LB medium slightly (data not shown). Consequently, estimates of reduced colonization by the mutant may be regarded as underestimates because without the GFP plasmid, the wild type would likely grow even faster.

ACKNOWLEDGMENTS. We thank Daniel M. Durachko and Ed Wagner for expert technical assistance and Dr. W. Schumann, University of Bayreuth, for the *B. subtilis* pMUTIN mutant. Use of the FIP/BM30a beamline of ESRF for the YoaJ (EXLX1) structure project was supported by the Fonds de la Recherche Scientifique under Contract IISN 4.4505.00. This work was supported by the European Commission Sixth Framework Program Grants LSMH-CT-COBRA 2003-503335 and LSMH-CT-EUR-INTAFAR 2004-512138; the Belgian Program on Interuniversity Poles of Attraction initiated by the Belgian State, Prime Minister's Office, Science Policy programming IAP no. P6/19; Actions de Recherche Concertées Grant 03/08-297; Fonds National de la Recherche Scientifique Grants 9.45/9.99, 2.4.508.01.F, 9.4.538.03.F, and 2.4.524.03; the University of Liège Fonds spéciaux, Crédit classique, 1999; and U.S. Department of Energy Grant DE-FG02-84ER13179 (to D.J.C.). F.K. is Chargé de Recherche of the Fonds de la Recherche Scientifique (F.R.S.-FNRS, Brussels, Belgium), and S.P. was a fellow of the French ''Fondation Recherche Médicale.''

1. Vollmer W, Joris B, Charlier P, Foster S (2008) Bacterial peptidoglycan (murein) hydrolases. *FEMS Microbiol Rev* 32:259–286.
2. Cosgrove DJ (2005) Growth of the plant cell wall. *Nat Rev Mol Cell Biol* 6:850–861.
3. Sampedro J, Cosgrove DJ (2005) The expansin superfamily. *Genome Biol* 6:242.
4. Cosgrove DJ (2000) Loosening of plant cell walls by expansins. *Nature* 407:321–326.
5. Yennawar NH, Li LC, Dudzinski DM, Tabuchi A, Cosgrove DJ (2006) Crystal structure and activities of EXPB1 (Zea m 1), a β-expansin and group-1 pollen allergen from maize. *Proc Natl Acad Sci USA* 103:14664–14671.
6. Carpita NC, Gibeaut DM (1993) Structural models of primary cell walls in flowering plants: Consistency of molecular structure with the physical properties of the walls during growth. *Plant J* 3:1–30.
7. Li Y, *et al*. (2002) Plant expansins are a complex multigene family with an ancient evolutionary origin. *Plant Physiol* 128:854–864.
8. Bais HP, Fall R, Vivanco JM (2004) Biocontrol of *Bacillus subtilis* against infection of *Arabidopsis* roots by *Pseudomonas syringae* is facilitated by biofilm formation and surfactin production. *Plant Physiol* 134:307–319.
9. Kende H, *et al*. (2004) Nomenclature for members of the expansin superfamily of genes and proteins. *Plant Mol Biol* 55:311–314.
10. Castillo RM, *et al*. (1999) A six-stranded double-psi β-barrel is shared by several protein superfamilies. *Structure* 7:227–236.
11. Madej T, Gibrat JF, Bryant SH (1995) Threading a database of protein cores. *Proteins* 23:356–369.
12. Li LC, Cosgrove DJ (2001) Grass group I pollen allergens (β-expansins) lack proteinase activity and do not cause wall loosening via proteolysis. *Eur J Biochem* 268:4217–4226.
13. Krissinel E, Henrick K (2004) Secondary-structure matching (SSM), a new tool for fast protein structure alignment in 3 dimensions. *Acta Crystallogr D* 60:2256–2268.
14. Emsley P, Cowtan K (2004) Coot: Model-building tools for molecular graphics. *Acta Crystallogr D* 60:2126–2132.
15. Ludvigsen S, Poulsen FM (1992) Three-dimensional structure in solution of barwin, a protein from barley seed. *Biochemistry* 31:8783–8789.
16. Davies GJ, Tolley SP, Henrissat B, Hjort C, Schulein M (1995) Structures of oligosaccharide-bound forms of the endoglucanase V from *Humicola insolens* at 1.9 A resolution. *Biochemistry* 34:16210–16220.
17. Eriksson J, *et al*. (2005) Model cellulose films exposed to *H. insolens* glucoside hydrolase family 45 endocellulase: The effect of the carbohydrate-binding module. *J Colloid Interface Sci* 285:94–99.
18. Hirvonen M, Papageorgiou AC (2003) Crystal structure of a family 45 endoglucanase from *Melanocarpus albomyces*: Mechanistic implications based on the free and cellobiose-bound forms. *J Mol Biol* 329:403–410.
19. Blackburn NT, Clarke AJ (2001) Identification of four families of peptidoglycan lytic transglycosylases. *J Mol Evol* 52:78–84.
20. van Straaten KE, Dijkstra BW, Vollmer W, Thunnissen AM (2005) Crystal structure of MltA from *Escherichia coli* reveals a unique lytic transglycosylase fold. *J Mol Biol* 352:1068–1080.
21. van Straaten KE, Barends TR, Dijkstra BW, Thunnissen AM (2007) Structure of *Escherichia coli* lytic transglycosylase MltA with bound chitohexaose: Implications for peptidoglycan binding and cleavage. *J Biol Chem* 282:21197–21205.
22. Boraston AB, Bolam DN, Gilbert HJ, Davies GJ (2004) Carbohydrate-binding modules: Fine-tuning polysaccharide recognition. *Biochem J* 382:769–781.
23. Cosgrove DJ, Bedinger P, Durachko DM (1997) Group I allergens of grass pollen as cell wall-loosening agents. *Proc Natl Acad Sci USA* 94:6559–6564.
24. Yuan S, Wu Y, Cosgrove DJ (2001) A fungal endoglucanase with plant cell wall extension activity. *Plant Physiol* 127:324–333.
25. Rose JK, Braam J, Fry SC, Nishitani K (2002) The XTH family of enzymes involved in xyloglucan endotransglucosylation and endohydrolysis: Current perspectives and a new unifying nomenclature. *Plant Cell Physiol* 43:1421–1435.
26. Doyle RJ, Koch AL (1987) The functions of autolysins in the growth and division of *Bacillus subtilis*. *Crit Rev Microbiol* 15:169–222.
27. Jolliffe LK, Doyle RJ, Streips UN (1981) The energized membrane and cellular autolysis in *Bacillus subtilis*. *Cell* 25:753–763.
28. Cavaglieri L, Orlando J, Rodriguez MI, Chulze S, Etcheverry M (2005) Biocontrol of *Bacillus subtilis* against *Fusarium verticillioides* in vitro and at the maize root level. *Res Microbiol* 156:748–754.
29. Gartemann KH, *et al*. (2003) *Clavibacter michiganensis* subsp *michiganensis*: First steps in the understanding of virulence of a Gram-positive phytopathogenic bacterium. *J Biotechnol* 106:179–191.
30. Laine MJ, *et al*. (2000) The cellulase encoded by the native plasmid of *Clavibacter michiganensis* ssp *sepedonicus* plays a role in virulence and contains an expansin-like domain. *Physiol Mol Plant Pathol* 57:221–233.
31. Brotman Y, Briff E, Viterbo A, Chet I (2008) Role of swollenin, an expansin-like protein from *Trichoderma*, in plant root colonization. *Plant Physiol* 147:779–789.
32. Ochiai A, Itoh T, Kawamata A, Hashimoto W, Murata K (2007) Plant cell wall degradation by saprophytic *Bacillus subtilis* strains: Gene clusters responsible for rhamnogalacturonan depolymerization. *Appl Environ Microbiol* 73:3803–3813.
33. Nooren IM, Thornton JM (2003) Structural characterization and functional significance of transient protein–protein interactions. *J Mol Biol* 325:991–1018.
34. McQueen-Mason SJ, Cosgrove DJ (1995) Expansin mode of action on cell walls: Analysis of wall hydrolysis, stress relaxation, and binding. *Plant Physiol* 107:87–100.
35. Vagner V, Dervyn E, Ehrlich SD (1998) A vector for systematic gene inactivation in *Bacillus subtilis*. *Microbiology* 144:3097–3104.
36. McQueen-Mason S, Durachko DM, Cosgrove DJ (1992) Two endogenous proteins that induce cell wall expansion in plants. *Plant Cell* 4:1425–1433.
37. Li LC, Bedinger PA, Volk C, Jones AD, Cosgrove DJ (2003) Purification and characterization of four β-expansins (Zea m 1 isoforms) from maize pollen. *Plant Physiol* 132:2073–2085.
38. Yaryura PM, *et al*. (2008) Assessment of the role of chemotaxis and biofilm formation as requirements for colonization of roots and seeds of soybean plants by *Bacillus amyloliquefaciens* BNM339. *Curr Microbiol* 56:625–632.

Supporting Information

Kerff *et al.* 10.1073/pnas.0809382105

Materials and Methods

Knockout of *yoaJ* Gene in *B. subtilis* 168. The *yoaJ* gene was amplified by PCR from *Bacillus subtilis* 168 1A1 genomic DNA, cloned into pGem-Teasy vector, and verified by sequencing. The plasmid was digested by BamHI restriction enzyme (*yoaJ* presents a unique BamHI recognition site at position 156) treated with alkaline phosphatase and ligated with BamHI-predigested mini Tn10, which contains a spectinomycin (Spc) cassette. The resultant plasmid bearing *yoaJ* interrupted by Tn10-Spc cassette was amplified in *Escherichia coli* Top10, purified (GFix mini-preparation kit; GE Biosciences), and digested by EcoRI to release the insert. The linear fragment containing *yoaJ-Spc* was purified and used to transform *B. subtilis*-competent cells. *B. subtilis* was made competent in MD medium [92% (wt/vol) glucose, 0.05 g/L L-Trp, 0.011 g/L ferric ammonium citrate, 2.5 g/L potassium aspartate, 0.36 g/L magnesium sulfate, 9.85 g/L dipotassium hydrogen phosphate, 5.5 g/L potassium dihydrogen phosphate, 0.92 g/L trisodium citrate). The resultant recombinants were selected on LB agar plates supplemented with 100 mg/L spectinomycin. Double recombination was verified by sequencing and Southern blotting. Complementation studies of the EXLX1$^-$ mutant were done by transforming *B. subtilis* 168 *yoaJ*$^-$ (*BsJ*$^-$) with the promoterless shuttle vector pCN35 (1), in which the complete *yoaJ* gene plus promoter region were cloned and verified by sequencing both DNA strands. The cloned fragment was obtained by PCR with Bs genomic DNA as matrix and primers UP-K 5′-GGTACCTGAGCCTGATTTTTATCACTTCAT-3′ and RP-S 5′-GTCGACAATGAGTTCATTCGGAACTAGAC-3′, which included KpnI and SalI restriction sites (underlined) for cloning.

Protein Purification. Recombinant EXLX1 was purified on a 150-mL S-Sepharose Fast Flow column with a 0–1 M NaCl elution gradient in a 50 mM Tris·HCl (pH 8) buffer followed by separation on a 150-mL QAE-Sepharose Fast Flow column with a 0–1 M NaCl elution gradient in a 50 mM Tris·HCl (pH 10.2) buffer. The protein was dialyzed against a 50 mM sodium phosphate (pH 7.0) buffer and stored at 4 °C. SeMet protein purification included 1 mM DTT in every buffer to prevent the oxidation of the SeMet.

Crystallization, Data Collection, Structure Solution, and Refinement. EXLX1 was concentrated to 46 mg/mL and crystallized at 20 °C by using the hanging-drop vapor diffusion method. Crystals used for data collection were obtained with a precipitating solution containing 4 M sodium formate and a 100 mM sodium acetate (pH 4.4) buffer. Crystals were transferred to a cryoprotectant solution containing 50% glycerol for freezing in liquid N_2 preceding data collection. The same procedure was used to obtained SeMet derivative crystals, except 5 mM DTT was included in the buffer.

All of the data were collected at the BM30A beamline of the European Synchrotron Radiation Facility. The dataset corresponding to the SeMet derivative was integrated and scaled with the programs Mosflm and Scala from the CCP4 suite (2). The crystals belong to the body centered cubic space group I23 with a unit cell axis length of 144.04 Å and are characterized by a very high solvent content (73%). The single-wavelength anomalous diffraction method was used to solve the structure with a 2.5-Å resolution dataset collected at the selenium absorption edge. The positions of 7 selenium atoms were identified and refined with occupancies >67% with the software Solve (3). By using the initial set of phases derived from those positions, the program Resolve (4) automatically built the backbone of 174 residues and the side chains of 29 of them. The subsequent refinement and model building cycles were performed with CNS (5) and O (6), respectively. All of the aa of the protein are modeled in the final structure, except the N-terminal SeMet.

A higher resolution model of this structure (1.9 Å) was obtained with the native (non-SeMet) protein. Data were integrated and scaled with the program XDS. The space group and unit cell parameters of the crystal are almost identical to the SeMet derivative. The refinement and model building cycles were performed with Refmac5 (7) and Coot (8), respectively. The coordinates and structure factors of the SeMet derivative and the native structures have been deposited in the Protein Data Bank with the respective PDB ID codes 2BH0 and 3D30. All of the images displaying crystallographic structures were made by using Pymol.

The contact area of domains interface was calculated as the average difference between the solvent-accessible surfaces of both domains on their own and the whole protein by using CCP4 (2).

Binding to Plant Cell Walls. Washed plant cell wall fragments were prepared from maize silks as described in ref. 9. Cell walls (3 mg) or cellulose (3 mg) from acid-washed cotton liners (Fluka no. 22184) were incubated with 20 μg of EXLX1 in 500 μL of 50 mM sodium acetate buffer (pH 5.5) for 1 h at 25 °C with agitation. Ovalbumin was included at 1 mg/mL as a nonspecific blocking agent. $CaCl_2$ at 10 mM was included in the buffer in some experiments. Samples were centrifuged to pellet the solid materials, and EXLX1 remaining in the supernatant was separated by reverse phase HPLC on a C8 column and quantified by 280-nm absorbance. Experiments were replicated 3 times with similar results.

Binding to Peptidoglycan. Peptidoglycan from *B. subtilis* 168 1A1 without teichoic acids was prepared as described in ref. 10. Pull-down assays were performed as follows. Twenty micrograms of purified EXLX1 was incubated on ice for 10 min with 3 mg of purified insoluble peptidoglycan from *B. subtilis* 168 1A1 in 500 μL of water. The samples were then centrifuged for 10 min at 13,000 $\times$ *g*, the supernatant was separated, and the pellet was washed once with 1 mL of water. The wash liquid was pooled with the first supernatant (sample 1). The pellet, consisting mostly of peptidoglycan, was further incubated for 10 min on ice with 500 μL of 5 M NaCl. The supernatant was recovered by centrifugation, and a second wash with 1 mL of the same solution was performed. Both supernatants were pooled (sample 2). The pellet was then incubated with 500 μL of 2% SDS at 100 °C for 5 min. The sample was centrifuged, supernatant recovered, and the treatment was repeated with 1 mL of 2% SDS. Both supernatants were pooled (sample 3). The pellet was then resuspended with 50 mM phosphate buffer (pH 7) and dialyzed overnight at 4 °C against the same buffer. The sample was adjusted to a 1.5-mL volume, 4 μg of lysozyme was added, and digestion proceeded overnight at 37 °C (sample 4). An equivalent volume of 300 μL for each sample (1 to 4) was concentrated, heated in denaturing buffer [10% glycerol, 2.5% 2-mercaptoethanol, 1% SDS, 31.25 mM Tris·HCl, 0.003% bromophenol blue (pH 6.8)], and samples were resolved by SDS/PAGE and estimated visually with Coomassie blue staining.

Lytic Activities. Two milligrams of dye-coupled cross-linked polysaccharide substrates (AZCL substrates; Megazyme) was suspended in 200 μL of Mes buffer (50 mM, pH 5.5) with 1 mM sodium azide to suppress microbial growth and incubated at 30 °C for 24 h with continuous shaking (1,000 rpm) with or without 27 μg of EXLX1. The reaction was stopped by the addition of 600 μL of 2.5% (wt/vol) Tris followed by centrifugation and measurement of the supernatant absorbance at 590 nm. AZLC substrates were prewashed extensively to reduce background, which varied among substrates. The reaction with rhamnogalacturonan used AZ-rhamnogalacturonan and was stopped by the addition of 600 μL of acetone. Independent experiments showed that protein purification fractions from empty pET vector controls (i.e., lacking EXLX1) had β(1–4)-D-endoglucanase activity (i.e., with cross-linked β-glucan and hydroxyethylcellulose) similar to that seen in purified EXLX1 fractions, suggesting that the latter had trace contamination with endogenous *E. coli* endoglucanase (data not shown).

Cellulose Hydrolysis. Five milligrams of Avicel (PH101, FMC Biopolymer) was incubated with agitation in 0.5 mL of 20 mM sodium acetate buffer (pH 5.5), with various protein additives, at 35 °C for 20 h. The samples were centrifuged to pellet the cellulose, and the supernatant was assayed for reducing sugars by PAHBAH assay (11). Additions included EXLX1 and BSA at 10 μg per tube, and 1 μg of crude *Trichoderma reesei* cellulase (Sigma C-8546).

Root Colonization. This assay was adapted from Yaryura *et al.* (12). Seeds of *Zea mays* were surface-disinfected in 3% sodium hypochlorite and germinated for 2 days at 28 °C in the dark, then transferred to culture tubes containing 5 mL of Murashige and Skoog (MS) mineral solution and a strip of filter paper as mechanical support of the seedling. Wild-type and mutant *B. subtilis* cultures were grown separately in LB medium overnight, washed twice, and resuspended in sterile MS medium. The tubes were inoculated with equal amounts of wild-type and mutant cells (0.25 mL titrated to 8×10^6 cfu mL^{-1}) or with 0.5 mL of MS for the controls. The seedlings were grown in an orbital shaker at 140 rpm in a plant-growth chamber under a 16 h/8 h light/dark cycle at 20 °C. A census of wild-type and mutant cells attached to the roots was made 3 days after inoculation. Wild-type cells carried a plasmid for expression of green fluorescent protein (GFP), making for easy visual distinction between wild-type and mutant colonies. Control experiments showed that the GPF plasmid slowed *B. subtilis* growth in LB medium slightly (data not shown). Consequently, estimates of reduced colonization by the mutant must be regarded as underestimates, because without the GFP plasmid the wild type would likely grow even faster. Seedlings were withdrawn from the tubes at day 3 and placed on sterile filter paper to remove excess medium. The plants were then submerged in 5 mL of sterile MS in new culture tubes and vortexed for 1 min to extract loosely bound bacteria, which were discarded. Roots were then sonicated (10 min) in a water-bath sonicator to remove tightly bound bacteria, which were serially diluted and plated on LB agar plates. Petri dishes were incubated for 24 h at 30 °C, and colonies were counted under a fluorescence microscope to distinguish wild-type (GFP-containing) from mutant colonies. Counts were expressed as cfu mL^{-1} for bacteria suspended in medium. This experiment was also carried out without the GFP plasmid; instead, erythromycin selection, conferred by the pMUTIN insertion into the *yoaJ* gene, was used to distinguish the resistant mutant from the sensitive wild type, with qualitatively similar results (data not shown).

1. Charpentier E, *et al.* (2004) Novel cassette-based shuttle vector system for Gram-positive bacteria. *Appl Environ Microbiol* 70:6076–6085.
2. Collaborative Computational Project Number 4 (1994) The CCP4 suite: Programs for protein crystallography. *Acta Crystallogr D* 50:760–763.
3. Terwilliger TC, Berendzen J (1999) Automated MAD and MIR structure solution. *Acta Crystallogr D* 55:849–861.
4. Terwilliger TC (2000) Maximum-likelihood density modification. *Acta Crystallogr D* 56:965–972.
5. Brunger AT, *et al.* (1998) Crystallography and NMR system: A new software suite for macromolecular structure determination. *Acta Crystallogr D* 54:905–921.
6. Jones TA, Zou JY, Cowan SW, Kjeldgaard M (1991) Improved methods for building protein models in electron density maps and the location of errors in these models. *Acta Crystallogr A* 47:110–119.
7. Murshudov GN, Vagin AA, Dodson EJ (1997) Refinement of macromolecular structures by the maximum-likelihood method. *Acta Crystallogr D* 53:240–255.
8. Emsley P, Cowtan K (2004) Coot: Model-building tools for molecular graphics. *Acta Crystallogr D* 60:2126–2132.
9. Yennawar NH, Li LC, Dudzinski DM, Tabuchi A, Cosgrove DJ (2006) Crystal structure and activities of EXPB1 (Zea m 1), a β-expansin and group-1 pollen allergen from maize. *Proc Natl Acad Sci USA* 103:14664–14671.
10. Girardin SE, *et al.* (2003) Nod1 detects a unique muropeptide from Gram-negative bacterial peptidoglycan. *Science* 300:1584–1587.
11. Lever M (1972) A new reaction for colorimetric determination of carbohydrates. *Anal Biochem* 47:273–279.
12. Yaryura PM, *et al.* (2008) Assessment of the role of chemotaxis and biofilm formation as requirements for colonization of roots and seeds of soybean plants by *Bacillus amyloliquefaciens* BNM339. *Curr Microbiol* 56:625–632.
13. Yuan S, Wu Y, Cosgrove DJ (2001) A fungal endoglucanase with plant cell wall extension activity. *Plant Physiol* 127:324–333.

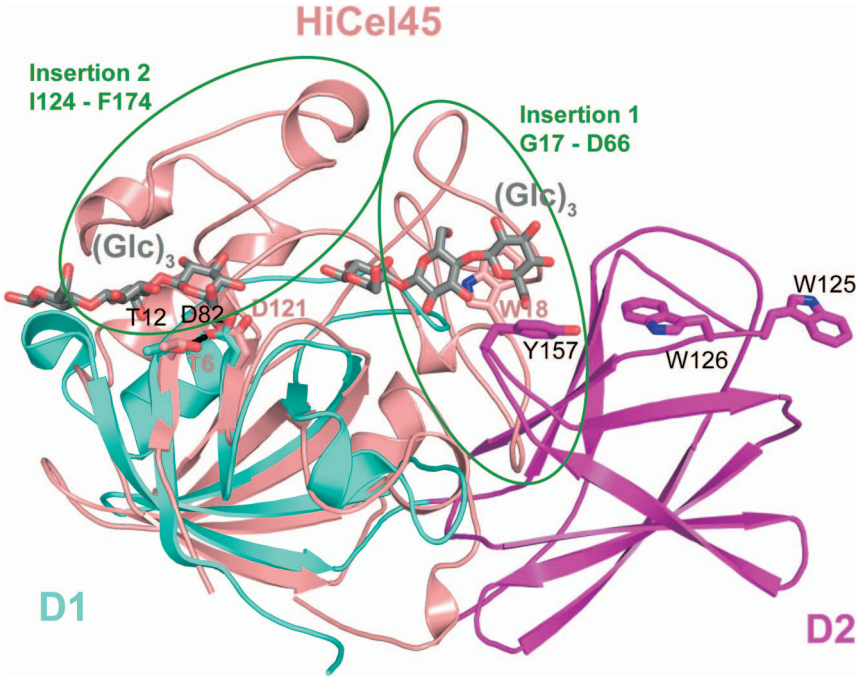

Fig. S1. Diagram representations of EXLX1 and the HiCel45–cellohexaose complex (peach, PDB ID code 4ENG) superimposed. The 2 fragments of cellohexaose [$(Glc)_3$] are shown as gray sticks. The 2 major insertions in HiCel45 compared with D1 of EXLX1 are circled in green. Note that the hydrophobic surface formed by Y157, W126, and W125 in D2 of EXLX1 are correctly positioned to extend the potential glucan-binding surface of D1.

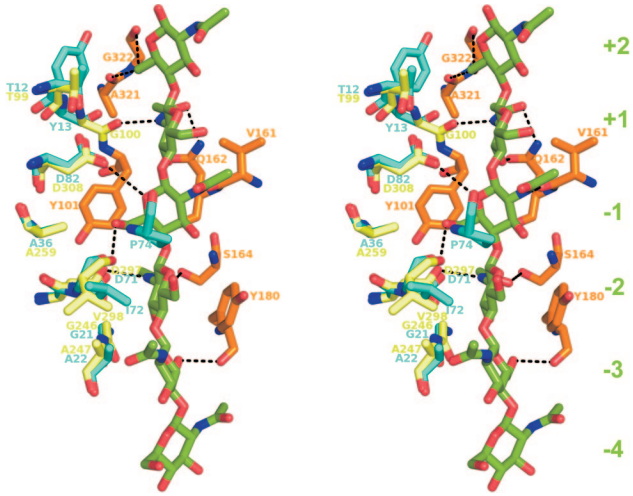

Fig. S2. Stereo stick representation of the active-site residues of the EcMltA(D308A)–chitohexahose complex superposed on EXLX1. The chitohexaose molecule is green, residues of EcMltA involved in the substrate binding and conserved in EXLX1 are yellow, and residues not conserved in EXLX1 are orange. D1 EXLX1 residues are cyan. Green numbers on the right numerate the residue-binding subsites. The peptidoglycan chain is a succession of GlcNAc and MurNAc units with a peptide bound to the lactate of the latter. In MltA, the different MurNAc units would occupy subsites +2, −1, and −3 because steric clashes would occur with a MurNAc lactate at the subsites +1 and −2. Steric clashes, however, less severe, might also happen in the same subsites of EXLX1. A similar binding mode of peptidoglycan to EXLX1 and MltA might therefore be expected.

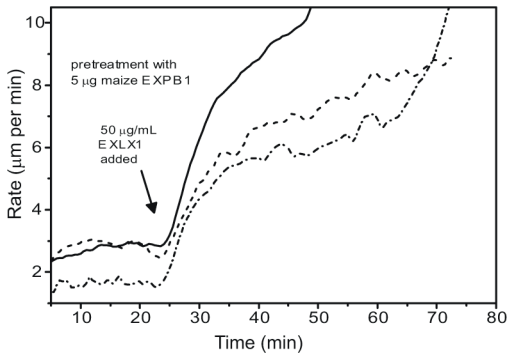

Fig. S3. Pretreatment of wheat coleoptile cell wall specimens with EXPB1 enhances subsequent extension induced by EXLX1. Three representative curves are shown in which heat-inactivated wall samples were pretreated with 5 μg/mL EXPB1 for 25 min followed by addition of EXLX1 to a final concentration of 50 μg/mL. The increase in extension rate was typically followed by cell wall breakage. When EXLX1 was given at this concentration without EXPB1, the extension response was $\approx$1 μm/min (see Fig. 3 *Inset*).

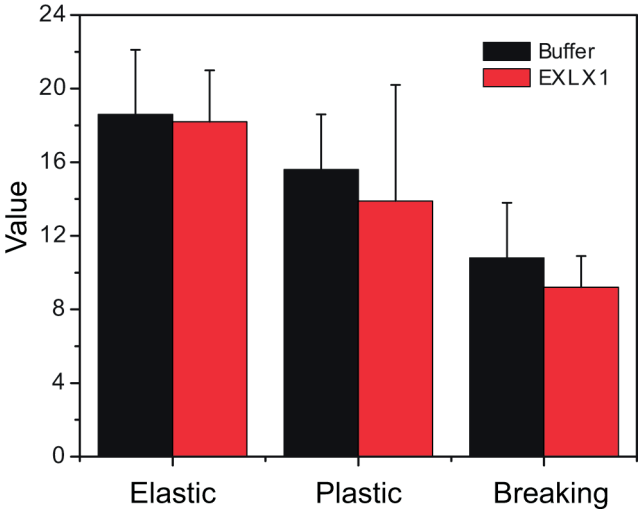

Fig. S4. Elastic and plastic compliances and breaking stresses of wheat coleoptile cell wall specimens. Heat-inactivated wall specimens from dark-grown wheat coleoptiles were prepared as described in ref. 13, preincubated for 4 h at 37 °C in 50 mM sodium acetate buffer (pH 4.5) with or without 250 μg/mL EXLX1, then a 5-mm segment was extended in a custom-built extensometer at 3 mm/min. Values are means ± SE of 15 samples. Elastic and plastic compliances were measured as described in ref. 13 and are expressed as percentage strain per 100 *g* force. To measure breaking strength, heat-inactivated wheat coleoptile walls were treated as above and then extended at a constant rate of 3 mm/min until they began to break. The maximum force (in grams) was taken as the breaking strength.

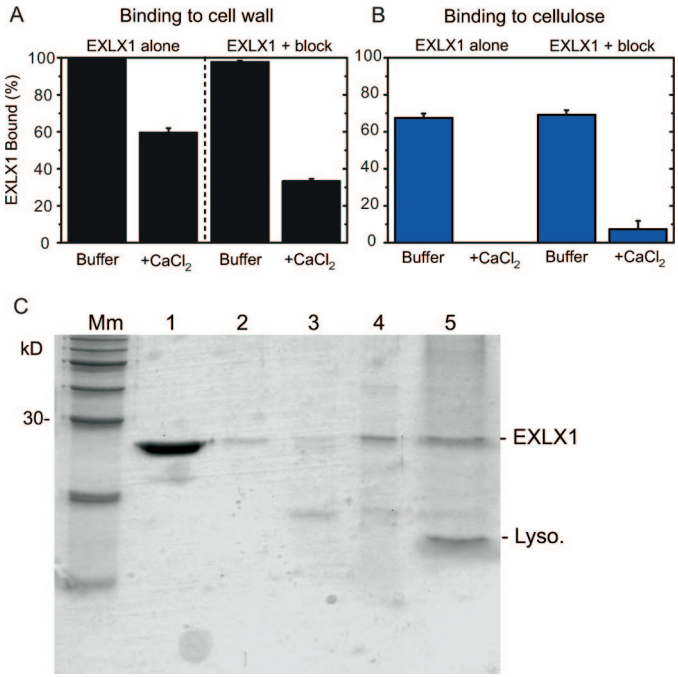

Fig. S5. EXLX1 binding to plant cell walls (*A*), cellulose (*B*), and peptidoglycan (*C*). (*A*) EXLX1 binding to maize cell walls is hardly affected by presence of 1 mg/mL ovalbumin as a blocking agent, but it is substantially reduced by the addition of 10 mM $CaCl_2$ to the buffer. (*B*) EXLX1 binding to cellulose is not reduced by the presence of 1 mg/mL ovalbumin as a blocking agent, but it is greatly reduced by the addition of 10 mM $CaCl_2$ to the buffer. (*C*) Binding of EXLX1 to *B. subtilis* peptidoglycan. Mm, molecular mass ladder. Lane 1, EXLX1 without peptidoglycan incubation; lane 2, soluble EXLX1 after incubation with peptidoglycan; lane 3, supernatant after 5 M NaCl wash of EXLX1–peptidoglycan complex; lane 4, supernatant after 2% SDS wash of EXLX1–peptidoglycan complex; lane 5, supernatant after lysozyme digestion of EXLX1–peptidoglycan complex. Data in *A* and *B* are means of 3 replicates ± standard errors.

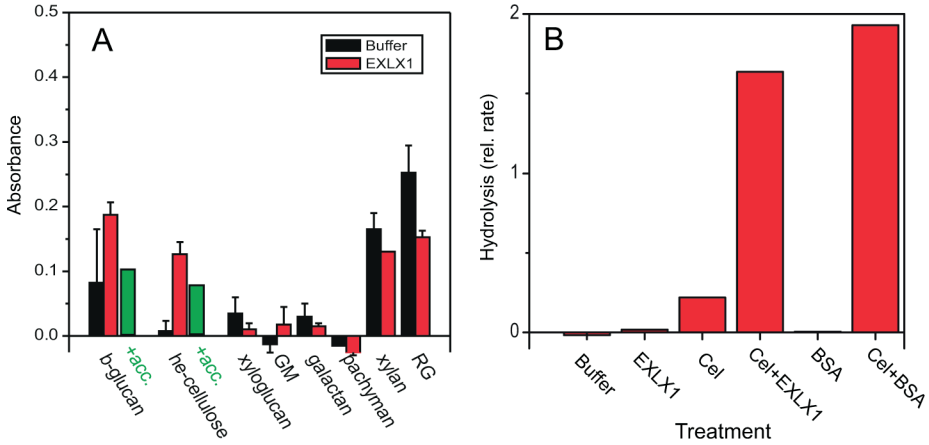

Fig. S6. Lytic activities of EXLX1 against plant cell wall polysaccharides. (*A*) Dye-coupled cross-linked substrate [2 mg in 200 μL of 50 mM Mes buffer (pH 5.5)] was incubated for 24 h with buffer alone (Control) or with the addition of 27 μg of EXLX1. Shown is the mean ± SEM of 2–4 replicates. Green bars (+acc): tubes were spiked with 0.5 mg of β(1–3,1–4)-D-glucan as a potential acceptor for transglycosylase activity. GM, galactomannan; RG, rhamnoglacturonan; he, hydroxyethyl; pachyman, β(1–3)-Dglucan. (*B*) EXLX1 nonspecifically enhances hydrolysis of cellulose (Avicel) by low amounts of cellulase. EXLX1 and BSA (10 μg) did not cause cellulose hydrolysis, but greatly enhanced the hydrolytic activity of small amounts (1 μg) of *Trichoderma* cellulase (Cel).

Table S1. Data collection and refinement statistics for two EXLX1 structures

Statistics	SeMet	Native
Diffraction data		
Space group	I23	I23
Unit cell parameters		
$a = b = c$, Å	144.04	143.78
$a = b = g$, °	90	90
Resolution range, Å	25.5–2.5 (2.64–2.5)	45.4–1.9 (2.0–1.9)
Measured reflections	755,962 (103,834)	582,394 (80,747)
Unique reflections	17,348 (2,505)	38,981 (5,607)
Completeness, %	99.9 (99.9)	99.8 (98.9)
Redundancy	21.8 (21.1)	14.9 (14.4)
R_{sym}, %*	13 (68)	16 (163)
R_{pim}, %†		4.1 (42.8)
Average I/σ	31.6 (5.1)	16.1 (2.0)
Refinement		
Resolution range, Å	25.5–2.5 (2.64–2.5)	45.4–1.9 (1.95–1.9)
No. of reflections	17,348 (2,505)	36,971 (2,760)
R_{cryst}, %‡	20 (30.3)	16.3 (30.6)
R_{free}, %§	23 (36.1)	19.1 (32.5)
rms deviations		
Bond length, Å	0.007	0.016
Bond angles, °	1.3	1.5
No. of residues	207	208
Mean B value		
Protein atoms, Å^2	32.7	35.9
Solvent atoms, Å^2	39.8	45.3
PDB ID code	2BH0	3D30

Values in parentheses correspond to the high-resolution shell.

*$R_{sym} = \Sigma\ (I - \langle I \rangle)/\Sigma\ I$; I is the intensity of an individual reflection, and $\langle I \rangle$ is the mean value of all of the measurements of that reflection.

†R_{pim}, Precision-indicating merging R factor.

‡$R_{cryst} = \Sigma\ |F_o - F_c|/\Sigma\ |F_o|$; F_o and F_c are, respectively, observed and calculated structure factors.

§R_{free} calculated for a randomly selected subset of reflections (5%) that were omitted during the refinement.

Table S2. Results of the pairwise superposition with the SSM algorithm of the 9 proteins that recognize polysaccharides and have an available crystallographic structure containing a double-ψ β−barrel fold

D1	BsEXLX1	EXPB1	Phl p 1	EcMltA	AtMltA	NgMltA	MeCel45A	HiCel45	MaCel45
BsEXLX1		98	96	83	80	78	89	83	85
EXPB1	1.9		117	104	95	93	96	82	85
Phl p 1	1.6	0.9		86	88	89	89	85	84
EcMltA	2.6	3.8	2.6		135**	135**	89	81	83
AtMltA	2.0	2.8	2.7	2.0**		164**	78	84	87
NgMltA	1.9	2.8	2.7	2.0**	1.5**		82	79	88
MeCel45A	2.0	2.4	2.0	3.1	2.7	2.8		106*	111*
HiCel45	2.3	1.9	2.0	2.8	3.1	2.6	2.2*		202*
MaCel45	2.1	2.1	1.9	2.8	2.9	2.9	2.2*	0.5*	

D1+D2	BsEXLX1	EXPB1	Phl p 1
BsEXLX1		186	181
EXPB1	2.3		209
Phl p 1	2.3	1.7	

D2	BsEXLX1	EXPB1	Phl p 1
BsEXLX1		82	83
EXPB1	1.6		87
Phl p 1	1.6	1.5	

	BsEXLX1	EXPB1	Phl p 1	EcMltA	AtMltA	NgMltA	MeCel45A	HiCel45	MaCel45
EXPB1	27.5								
Phl p 1	23.9	62.4							
EcMltA	14.4	11.5	15.1						
AtMltA	10.0	8.4	12.5	26.7**					
NgMltA	15.4	14.0	15.7	30.4**	32.9**				
MeCel45A	18.0	21.9	22.5	9.0	9.0	13.4			
HiCel45	19.3	26.8	25.8	11.1	8.3	12.7	21.7*		
MaCel45	10.6	23.5	23.8	13.2	11.5	11.4	21.6*	78.7*	

D1+D2	BsEXLX1	EXPB1	Phl p 1
EXPB1	22.5		
Phl p 1	22	58.3	

D2	BsEXLX1	EXPB1	Phl p 1
EXPB1	22.0		
Phl p 1	21.7	54.0	

 # residues **rmsd** **% identity**

* calculated for the whole proteins

** calculated with the N-terminal extension of the different MltA included

Rmsd is highlighted in green, the number of residues included in the rmsd calculation is in orange, and the percentage of sequence identity is in pink.

Table S3. Summary of results of BLAST using EXLX1 as query

Sequences producing significant alignments	Score, bits	*E* value
gi | 16078923 | ref | NP_389744.1 | Hypothetical protein BSU18630 [B. . .	468	7e-131
gi | 110590882 | pdb | 2BH0 | A chain A, crystal structure of a semet. . .	400	2e-110
gi | 52080641 | ref | YP_079432.1 | YoaJ [*Bacillus licheniformis* ATC. . .	395	6e-109
gi | 21232964 | ref | NP_638881.1 | Cellulase [*Xanthomonas campestri*. . .	297	2e-79
gi | 84625463 | ref | YP_452835.1 | Cellulase [*Xanthomonas oryzae* pv. . .	286	5e-76
gi | 58583659 | ref | YP_202675.1 | Cellulase [*Xanthomonas oryzae* pv. . .	286	8e-76
gi | 71275113 | ref | ZP_00651400.1 | Glycoside hydrolase, family 5:. . .	278	2e-73
gi | 71899133 | ref | ZP_00681297.1 | Glycoside hydrolase, family 5:. . .	277	3e-73
gi | 28199725 | ref | NP_780039.1 | Extracellular endoglucanase prec. . .	277	3e-73
Gi | 15837412 | ref | NP_298100.1 | Extracellular endoglucanase prec. . .	275	1e-72
Gi | 83747707 | ref | ZP_00944742.1 | Hypothetical protein RRSL_0239. . .	263	7e-69
gi | 50121146 | ref | YP_050313.1 | Putative cellulase [*Erwinia caro*. . .	260	3e-68
gi | 17545537 | ref | NP_518939.1 | PUTATIVE ENDOGLUCANASE PROTEIN [. . .	252	1e-65
gi | 115373847 | ref | ZP_01461139.1 | YoaJ [*Stigmatella aurantiaca* . . .	159	8e-38
gi | 118062185 | ref | ZP_01530535.1 | Rare lipoprotein A [*Roseiflex*. . .	159	1e-37
gi | 106889938 | ref | ZP_01357135.1 | Rare lipoprotein A [*Roseiflex*. . .	158	2e-37
gi | 76260027 | ref | ZP_00767669.1 | Rare lipoprotein A [*Chloroflex*. . .	141	2e-32
gi | 108762346 | ref | YP_631763.1 | Putative lipoprotein [*Myxococcu*. . .	124	3e-27
gi | 68227444 | ref | ZP_00566650.1 | Rare lipoprotein A [*Frankia* sp. . .	120	4e-26
gi | 113941594 | ref | ZP_01427385.1 | Rare lipoprotein A [*Herpetosi*. . .	110	4e-23
gi | 13277513 | gb | AAK16222.1 | cellulase CelA [*Clavibacter michigane*	104	3e-21
gi | 8980306 | emb | CAA44467.2 | Cellulase [*Clavibacter michiganensis*]	95.9	2e-18
gi | 115377675 | ref | ZP_01464869.1 | cellulase [*Stigmatella aurant*. . .	95.5	2e-18
gi | 83646399 | ref | YP_434834.1 | Endoglucanase C-terminal domain/. . .	92.4	1e-17
gi | 119479709 | ref | XP_001259883.1 | Extracellular cellulase CelA. . .	89.4	1e-16
gi | 70998214 | ref | XP_753833.1 | Cellulase CelA [*Aspergillus fumi*. . .	87.8	4e-16

The highest hits (with scores above 250 bits, upper half of table) are from bacteria that colonize plant root surfaces or are plant pathogens that reside in plant vascular systems.